Article:
Chittock, J. orcid.org/0000-0002-1595-7441, Cork, M.J. orcid.org/0000-0003-4428-2428 and Danby, S.G. orcid.org/0000-0001-7363-140X (2022) Real-Time Infrared spectroscopic measurement of natural moisturising factor. Journal of Investigative Dermatology, 143 (4). 676-679.e5. ISSN 0022-202X

https://doi.org/10.1016/j.jid.2022.10.005

***Yan Zheng*[1,2,6], *Jie Yao*[3,6], *Xiner Shen*[3], *Haijun Cheng*[3], *Yinbo Peng*[4], *Weiqiang Tan*[2], *Michael P. Timko*[5] and *Longjiang Fan*[3,*]**

[1]*Department of Plastic Surgery, The Quzhou Affiliated Hospital of Wenzhou Medical University and Quzhou People's Hospital, Quzhou, China;* [2]*Department of Plastic Surgery, Sir Run Run Shaw Hospital, School of Medicine, Zhejiang University, Hangzhou, China;* [3]*Institute of Bioinformatics, Zhejiang University, Hangzhou, China;* [4]*Department of Plastic and Reconstructive Surgery, The 9th People's Hospital Affiliated to Shanghai Jiao Tong University School of Medicine, Shanghai, China; and* [5]*Department of Public Health Sciences, School of Medicine, University of Virginia, Charlottesville, Virginia, USA*
[6]*These authors contributed equally to this work.*
[*]*Corresponding author e-mail: fanlj@zju.edu.cn*

SUPPLEMENTARY MATERIAL

Supplementary material is linked to the online version of the paper at www.jidonline.org, and at https://doi.org/10.1016/j.jid.2022.10.008

REFERENCES

Deng CC, Hu YF, Zhu DH, Cheng Q, Gu JJ, Feng QL, et al. Single-cell RNA-seq reveals fibroblast heterogeneity and increased mesenchymal fibroblasts in human fibrotic skin diseases. Nat Commun 2021;12:3709.

Direder M, Weiss T, Copic D, Vorstandlechner V, Laggner M, Pfisterer K, et al. Schwann cells contribute to keloid formation. Matrix Biol 2022;108:55–76.

Franzén O, Gan LM, Björkegren JLM. PanglaoDB: a web server for exploration of mouse and human single-cell RNA sequencing data. Database (Oxford) 2019;2019. baz046.

Griffin MF, Borrelli MR, Garcia JT, Januszyk M, King M, Lerbs T, et al. JUN promotes hypertrophic skin scarring via CD36 in preclinical in vitro and in vivo models. Sci Transl Med 2021;13:eabb3312.

Liu X, Chen W, Zeng Q, Ma B, Li Z, Meng T, et al. Single-cell RNA-sequencing revealslineage-specific regulatory changes of fibroblasts and vascular endothelial cells in keloids. J Invest Dermatol 2022;142:124–135.e11.

Mascharak S, desJardins-Park HE, Davitt MF, Griffin M, Borrelli MR, Moore AL, et al. Preventing Engrailed-1 activation in fibroblasts yields wound regeneration without scarring. Science 2021;372:eaba2374.

Shim J, Oh SJ, Yeo E, Park JH, Bae JH, Kim SH, et al. Integrated analysis of single-cell and spatial transcriptomics in keloids: highlights on fibrovascular interactions in keloid pathogenesis. J Invest Dermatol 2022;142:2128–2139.e11.

Solé-Boldo L, Raddatz G, Schütz S, Mallm JP, Rippe K, Lonsdorf AS, et al. Single-cell transcriptomes of the human skin reveal age-related loss of fibroblast priming. Commun Biol 2020;3:188.

Sun Y, Hu Y, Zhang Y, Wei S, Yang B, Xu Y, et al. FibROAD: a manually curated resource for multi-omics level evidence integration of fibrosis research. Database 2022;2022:baac015.

Tabib T, Morse C, Wang T, Chen W, Lafyatis R. SFRP2/DPP4 and FMO1/LSP1 define major fibroblast populations in human skin [published correction appears in J Invest Dermatol 2018;138:2086] J Invest Dermatol 2018;138:802–10.

Theocharidis G, Tekkela S, Veves A, McGrath JA, Onoufriadis A. Single-cell transcriptomics in human skin research: available technologies, technical considerations and disease applications. Exp Dermatol 2022;31:655–73.

Trace AP, Enos CW, Mantel A, Harvey VM. Keloids and hypertrophic scars: a spectrum of clinical challenges. Am J Clin Dermatol 2016;17:201–23.

Vorstandlechner V, Laggner M, Copic D, Klas K, Direder M, Chen Y, et al. The serine proteases dipeptidyl-peptidase 4 and urokinase are key molecules in human and mouse scar formation. Nat Commun 2021;12:6242.

Yanai H, Budovsky A, Tacutu R, Barzilay T, Abramovich A, Ziesche R, et al. Tissue repair genes: the TiRe database and its implication for skin wound healing. Oncotarget 2016;7:21145–55.

Zhang X, Lan Y, Xu J, Quan F, Zhao E, Deng C, et al. CellMarker: a manually curated resource of cell markers in human and mouse. Nucleic Acids Res 2019;47:D721–8.

Real-Time Infrared Spectroscopic Measurement of Natural Moisturizing Factor

Journal of Investigative Dermatology (2023) **143,** 676–679; doi:10.1016/j.jid.2022.10.005

TO THE EDITOR

The quantification of natural moisturizing factor (NMF) is of value to scientists and clinicians with an interest in dry skin disorders such as atopic dermatitis (AD). Hygroscopic amino acids and their derivatives, originating from FLG catabolism, represent a predominant component of NMF maintaining the physical permeability barrier of the skin (Scott et al., 1982), that when deficient are synonymous with xerosis and greater AD severity (Horii et al., 1989; Nouwen et al., 2020). Tape stripping with chromatography is a fully quantitative assessment of NMF ex vivo but is time consuming and labor intensive in larger cohorts. In this pilot study, we tested a portable, handheld Attenuated Total Reflectance Fourier Transform Infrared (ATR-FTIR) spectrometer as an alternative in vivo measure of NMF by modeling chemometric absorption using a single, quantitative composite value obtained by established ex vivo laboratory assay. The spectroscopic model was verified by examining known scenarios of reduced NMF abundance in the skin such as the established FLG pathophysiology in AD.

A cohort of 26 participants with healthy skin (n = 15) or a history of AD (n = 11; two with mild active disease) were recruited and completed the single study visit. Written, informed consent was obtained, and approval was granted by the University of Sheffield Research Ethics Committee (reference 021945). Four sampling data points across the antecubital fossa and forearm were split equally between model calibration and validation, each consisting of four baseline ATR-FTIR measurements performed contiguously to three serial tape strips collected in duplicate (n = 6) for laboratory NMF analysis (Supplementary Figure S1). On average, the three predominant components of NMF analyzed ex vivo—total free amino acid pool, pyrrolidone carboxylic acid, and urocanic

Abbreviations: AD, atopic dermatitis; ATR-FTIR, Attenuated Total Reflectance Fourier Transform Infrared Spectroscopy; NMF, natural moisturizing factor

Accepted manuscript published online 8 November 2022; corrected proof published online 21 December 2022

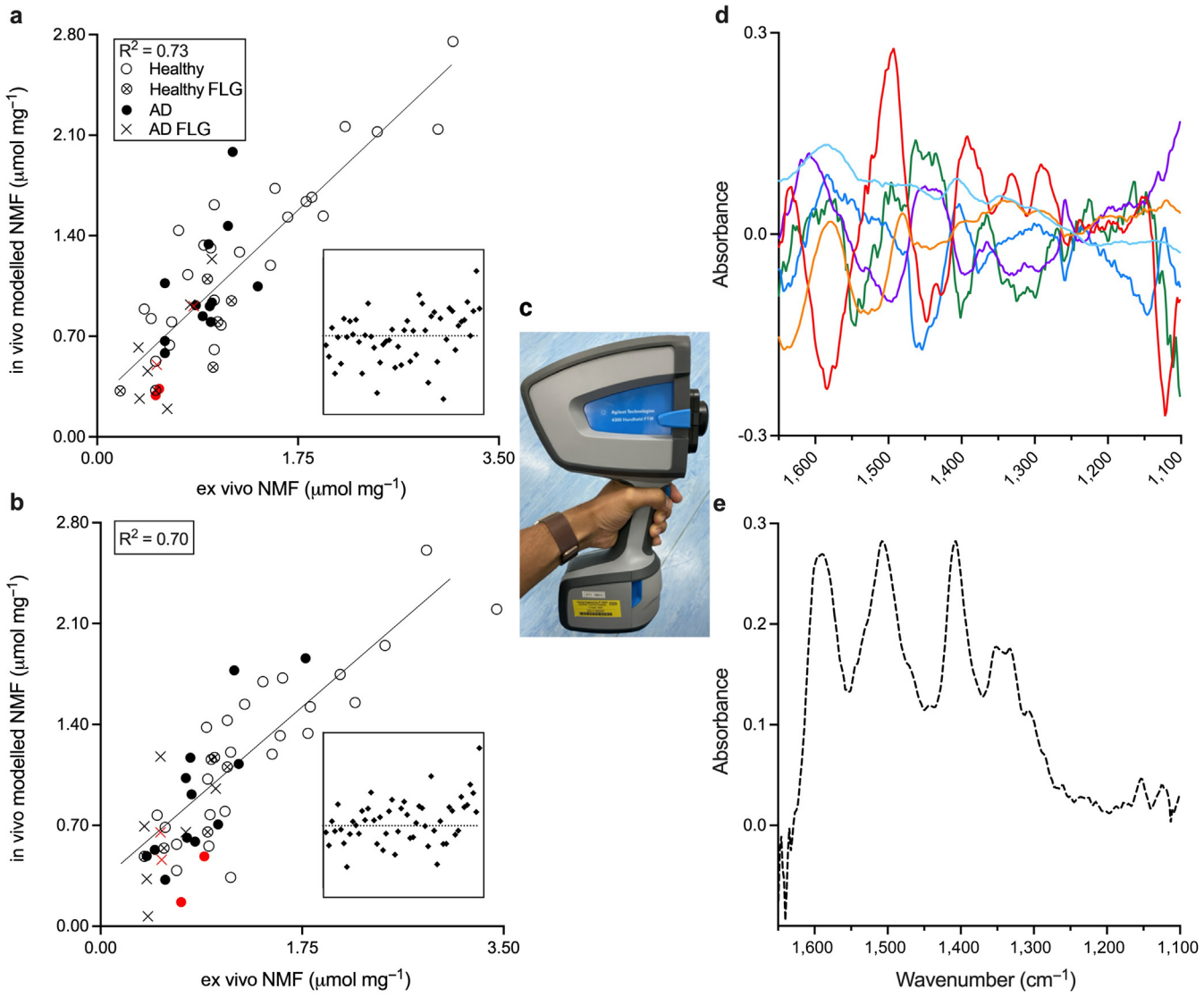

Figure 1. PLS chemometric modeling of surface NMF in the mid-infrared spectral region. (**a**) Plot of ex vivo quantified versus in vivo ATR-FTIR–modeled NMF (the sum of fAA, PCA, and UCA) for calibration and (**b**) validation data sets (see Supplementary Materials and Methods for further details). R^2 = coefficient of determination denoting linear regression model goodness of fit. Respective residual plots inset. Individuals with active AD are shaded red. (**c**) Image of the spectrometer used. (**d**) Loading plot associating wavenumber absorption to latent factor (six in total, color coded) with (**e**) an in vitro NMF absorbance spectrum presented for reference. AD, atopic dermatitis; ATR-FTIR, Attenuated Total Reflectance Fourier Transform Infrared Spectroscopy; fAA, free amino acid pool; NMF, natural moisturizing factor; PCA, pyrrolidone carboxylic acid; PLS, partial least squares; UCA, urocanic acid.

acid—were significantly reduced in the AD group compared to healthy skin (Supplementary Table S1). Transepidermal water loss and capacitance measurements to assess barrier function were similar between groups, and the proportions of *FLG* loss-of-function variants were 20 and 36% respectively. A plot of ex vivo versus in vivo modeled NMF is presented in Figure 1a and b. Using a six-factor predictive model, the coefficient of determination for calibration (R^2 = 0.73) and validation (R^2 = 0.70) sampling data points indicate satisfactory accuracy and precision (±0.35 μmoles mg^{-1}) denoted by the root mean square error of calibration. A plot of model loading—the strength of association between wavenumber absorption and latent factor (Figure 1d)—corresponded to an in vitro NMF profile collected by the same spectrometer (Figure 1c and e). Similar outputs were obtained by amide I (1,640 cm^{-1}) and amide II (1,540 cm^{-1}) normalization (Supplementary Table S2). To verify the spectroscopic technique, NMF was modeled before and after bathing the antecubital fossa in an independent cohort of volunteers (n = 5) (Supplementary Figure S2a), with on average, a 67% reduction in NMF induced by a 20-minute water soak (P = 0.0036). Furthermore, the main study cohort (n = 26) was stratified in two ways (healthy skin/AD and wild type/*FLG* loss-of-function variants) and the modeled NMF abundance compared, to assess the inherited and acquired FLG defect (Kezic et al., 2011). In all scenarios, similar changes in absorbance were observed that matched an in vitro NMF spectrum (Supplementary Figure S2b–h). These regions were indicative of the carboxylate (-COO$^-$) asymmetric or symmetric stretch (1,580/1,400 cm^{-1}) and methylene group (CH_2) vibrations around 1,480 cm^{-1} (Takada et al., 2012). Interestingly, 1,340 cm^{-1} is assigned to the hydroxyl group (C-OH) bending mode of

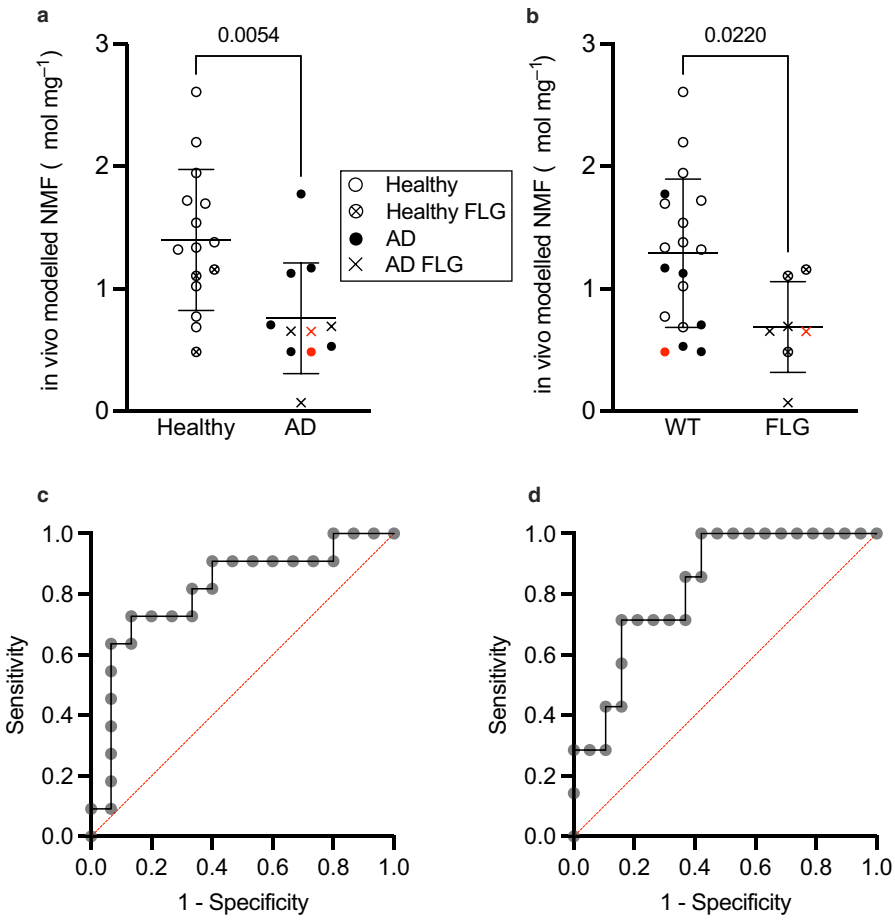

Figure 2. In vivo modeled NMF discriminates AD and *FLG* null genotypes from controls. Cohort stratification (n = 26) to compare mean in vivo NMF at the antecubital fossa between (**a**) healthy skin/AD and (**b**) WT/*FLG* LOF variants. Only the model validation data points are presented (see Supplementary Materials and Methods for further details). Individuals with active AD are shaded red. *P*-values denote the result of an unpaired Student's *t* test. A ROC curve of modeled NMF is presented below the corresponding graph. (**c**) AD/healthy: area under the curve = 0.81, 95% CI = 0.63–0.99, $P = 0.008$. (**d**) FLG/WT: area under the curve = 0.83, 95% CI = 0.66–0.99, $P = 0.01$). AD, atopic dermatitis; LOF, loss-of-function; NMF, natural moisturizing factor; ROC, receiver operating characteristic; WT, wild type.

serine, an abundant amino acid within the stratum corneum (Nakagawa et al., 2011). At the antecubital fossa but not the forearm (Supplementary Figure S3a and b), in vivo modeled NMF was on average 0.64 μmol mg^{-1} lower in AD than in healthy skin, with all values measured in *FLG* loss-of-function variants being below the wild-type mean, regardless of AD history (Figure 2a and b). This discrimination between groups was supported by a receiver operating characteristic area under the curve of 0.81 and 0.83, respectively (Figure 2c and d).

This methodology was limited to the discrimination of subclinical AD and requires further validation owing to the absence of more active disease. Compare this with in vivo Raman Spectroscopy where a more comprehensive classification of *FLG* genotype by NMF (area under the curve = 0.94) was reported in adults with moderate–severe disease (O'Regan et al., 2010). Our work is ongoing to replicate this ATR-FTIR methodology in a more diverse AD cohort of greater severity, but a key limitation may be the shallow sampling depth (approximately 1.5 μm) of the evanescent wave (Brancaleon et al., 2001), whereas Raman Spectroscopy permits composite NMF profiling across the full stratum corneum depth without the requirement of tape stripping. This surface constraint may also render the current ATR-FTIR methodology susceptible to patients washing or applying topical treatments before measurements in the clinic. On the flip side, it can be argued that ATR-FTIR is comparatively the more affordable technology that permits the rapid sampling of multiple anatomical sites, with a real-time NMF output displayed by the device.

In summary, we provide preliminary evidence to suggest that the measurement of NMF in vivo using ATR-FTIR is robust and comparable with an established ex vivo technique. Considering the portable device used with no sample preparation required, this methodology has the potential to offer new opportunities for clinical research where laboratory access is not feasible. The technology has many potential uses; knowledge of *FLG* variant status may predict a patient's response to emollients (Danby et al., 2022) or systemic immunosuppressives (Roekevisch et al., 2017) indicative of future personalized treatment strategies. Our data is also suggestive of attenuated NMF in patients generally clear of symptoms (Engebretsen et al., 2018). Tracking this defect longitudinally with further novel measures of subclinical inflammation may be of clinical value for monitoring remission post treatment of active disease (Byers et al., 2018). Another use is in predisposed neonates who possess a skin barrier defect long before the onset of clinical AD (Horimukai et al., 2016). There is evidence to suggest that low NMF associates with skin barrier breakdown at birth (Chittock et al., 2016). Therefore, as presented by this study in adults with unaffected skin, the hypothesis that NMF abundance may also be discriminative in neonates and predictive of AD onset either alone, or in conjunction with other biomarkers is an intriguing proposition yet to be determined.

Data availability statement

No large datasets were generated by this study.

ORCIDs

John Chittock: http://orcid.org/0000-0002-1595-7441
Michael J. Cork: http://orcid.org/0000-0003-4428-2428
Simon G. Danby: http://orcid.org/0000-0001-7363-140X

CONFLICT OF INTEREST

The authors state no conflict of interest.

ACKNOWLEDGMENTS

This study was funded by the LEO Foundation awards LF16062 and LF18005. We are very grateful to our volunteers for their participation, without which the study would not be possible. Many thanks to Rob Hanson of the Department of Chemistry for his assistance with high-performance liquid chromatography. We would also like to thank Leung Tang, Graham Miller, and Alexandra Harvey at Agilent Technologies for sharing expertise in infrared spectroscopy and providing access to Agilent's proprietary prototype 3B2P sampling interface. Figures were produced using Biorender.com and GraphPad Prism 9 (GraphPad Software, San Diego, CA).

AUTHOR CONTRIBUTIONS

Conceptualization: JC, MJC, SGD; Data Curation: MJC, SGD; Formal Analysis: JC, SGD; Funding Acquisition: MJC, SGD; Investigation: JC; Methodology: JC, SGD; Project Administration: JC, SGD; Resources: MJC, SGD; Supervision: MJC, SGD; Writing – Original Draft Preparation: JC; Writing – Review and Editing: JC, MJC, SGD

***John Chittock*[1,*], *Michael J. Cork*[1,2] *and Simon G. Danby*[1]**

[1]*Sheffield Dermatology Research, The Medical School, University of Sheffield, Sheffield, United Kingdom; and* [2]*The Paediatric Dermatology Clinic, Sheffield Children's Hospital, Sheffield, United Kingdom*

[*]*Corresponding author e-mail: j.chittock@sheffield.ac.uk*

SUPPLEMENTARY MATERIAL

Supplementary material is linked to the online version of the paper at www.jidonline.org, and at https://doi.org/10.1016/j.jid.2022.10.005.

REFERENCES

Brancaleon L, Bamberg MP, Sakamaki T, Kollias N. Attenuated total reflection-Fourier transform infrared spectroscopy as a possible method to investigate biophysical parameters of stratum corneum in vivo. J Invest Dermatol 2001;116:380–6.

Byers RA, Maiti R, Danby SG, Pang EJ, Mitchell B, Carré MJ, et al. Sub-clinical assessment of atopic dermatitis severity using angiographic optical coherence tomography. Biomed Opt Express 2018;9:2001–17.

Chittock J, Cooke A, Lavender T, Brown K, Wigley A, Victor S, et al. Development of stratum corneum chymotrypsin-like protease activity and natural moisturizing factors from birth to 4 weeks of age compared with adults. Br J Dermatol 2016;175:713–20.

Danby SG, Andrew PV, Taylor RN, Kay LJ, Chittock J, Pinnock A, et al. Different types of emollient cream exhibit diverse physiological effects on the skin barrier in adults with atopic dermatitis. Clin Exp Dermatol 2022;47:1154–64.

Engebretsen KA, Bandier J, Kezic S, Riethmüller C, Heegaard NHH, Carlsen BC, et al. Concentration of filaggrin monomers, its metabolites and corneocyte surface texture in individuals with a history of atopic dermatitis and controls. J Eur Acad Dermatol Venereol 2018;32:796–804.

Horii I, Nakayama Y, Obata M, Tagami H. Stratum corneum hydration and amino acid content in xerotic skin. Br J Dermatol 1989;121:587–92.

Horimukai K, Morita K, Narita M, Kondo M, Kabashima S, Inoue E, et al. Transepidermal water loss measurement during infancy can predict the subsequent development of atopic dermatitis regardless of filaggrin mutations. Allergol Int 2016;65:103–8.

Kezic S, O'Regan GM, Yau N, Sandilands A, Chen H, Campbell LE, et al. Levels of filaggrin degradation products are influenced by both filaggrin genotype and atopic dermatitis severity. Allergy 2011;66:934–40.

Nakagawa N, Naito S, Yakumaru M, Sakai S. Hydrating effect of potassium lactate is caused by increasing the interaction between water molecules and the serine residue of the stratum corneum protein. Exp Dermatol 2011;20:826–31.

Nouwen AEM, Karadavut D, Pasmans SGMA, Elbert NJ, Bos LDN, Nijsten TEC, et al. Natural Moisturizing Factor as a clinical marker in atopic dermatitis. Allergy 2020;75:188–90.

O'Regan GM, Kemperman PM, Sandilands A, Chen H, Campbell LE, Kroboth K, et al. Raman profiles of the stratum corneum define 3 filaggrin genotype-determined atopic dermatitis endophenotypes. J Allergy Clin Immunol 2010;126:574–580.e1.

Roekevisch E, Leeflang MMG, Schram ME, Campbell LE, Irwin McLean WH, Kezic S, et al. Patients with atopic dermatitis with filaggrin loss-of-function mutations show good but lower responses to immunosuppressive treatment. Br J Dermatol 2017;177:1745–6.

Scott IR, Harding CR, Barrett JG. Histidine-rich protein of the keratohyalin granules. Source of the free amino acids, urocanic acid and pyrrolidone carboxylic acid in the stratum corneum. Biochim biophys acta 1982;719:110–7.

Takada S, Naito S, Sonoda J, Miyauchi Y. Noninvasive in vivo measurement of natural moisturizing factor content in stratum corneum of human skin by attenuated total reflection infrared spectroscopy. Appl Spectrosc 2012;66:26–32.

Macrophage Migration Inhibitory Factor Restriction of HIV-1 Transinfection from Dendritic Cells to CD4+ T Cells through the Regulation of Autophagy

Journal of Investigative Dermatology (2023) **143,** 679–682; doi:10.1016/j.jid.2022.09.655

TO THE EDITOR

At mucosal surfaces, immature resident dendritic cells (DCs) and Langerhans cells (LCs) are among the first cell types to encounter and be infected by HIV-1 virus (Ahmed et al., 2015; Pena-Cruz et al., 2018). LCs and myeloid DCs can restrict early HIV-1 infection through active mechanisms of viral entry restriction owing to their primary autophagic functions (Blanchet et al., 2010). During early-stage infection, the recognition of virus by DCs results in the release of cytokines: IFN-stimulated genes and TGF-β have shown their contribution to the control of HIV-1 infection (Czubala et al., 2016; Soper et al., 2017). Cell-to-cell models of early HIV-1 infection have established the role of DCs in HIV-1 transfer to T lymphocytes (Garcia et al., 2005).

To better understand the contribution of cytokines in the regulation of HIV-1 transinfection, we performed a small interfering RNA (siRNA) screen in monocyte-derived DCs (MDDCs) in a DC-to-CD4+ T cell transfer system and monitored the transfer of HIV-1 in CD4+ T cells. Using the Dharmacon

Abbreviations: CQ, chloroquine; DC, dendritic cell; LC, Langerhans cell; MDDC, monocyte-derived dendritic cell; MIF, migration inhibitory factor; siRNA, small interfering RNA

Accepted manuscript published online 17 October 2022; corrected proof published online 12 January 2023

SUPPLEMENTARY MATERIALS AND METHODS

Participants

A cohort study was designed to compare surface NMF levels between volunteers with either atopic dermatitis or healthy skin using a portable infrared specrometer for in vivo quantification. Volunteers were recruited from the local community of the city of Sheffield, United Kingdom between November 2017 and October 2018. A diagnosis of atopic dermatitis was made using the United Kingdom working party criteria (Williams et al., 1994). Healthy volunteers had no history of skin disease. An additional cohort of five healthy volunteers was recruited to investigate the effect of a short water soak (20 minutes, 1 ml distilled water warmed to 37 ºC contained by an open chamber) on NMF. All volunteers were asked not to apply any topical products or shower on the morning of the study visit.

Skin assessments

All skin assessments were performed during a single visit to our dedicated, climate-controlled skin barrier suite located at the University of Sheffield (Sheffield, United Kingdom). Room conditions were maintained at 20 ± 2 °C and 38–50% relative humidity. The volar aspect of the forearm and the antecubital fossa were the designated study sites. The Eczema Area and Severity Index score was employed as a measure of atopic dermatitis severity. Transepidermal water loss was assessed using an AquaFlux AF200 closed chamber condensing device (Biox Systems, London, United Kingdom). Skin capacitance was measured using a Corneometer CM825 probe (Courage+Khazaka electronic GmbH, Cologne, Germany). Volunteers acclimatized to the room conditions for 20 minutes before assessment.

Infrared spectroscopy

A portable 4300 handheld Fourier Transform Infrared spectrometer with mercury cadmium telluride detector (Agilent Technologies, Santa Clara, CA) was equipped with a 3-bounce/two-pass diamond Attenuated Total Reflectance accessory to collect absorption spectra at the skin surface in the mid-infrared region from 32 scans at 4 cm^{-1} resolution. The area of the sampling probe that contacts the skin is approximately 79 mm^2.

NMF laboratory analysis ex vivo by tape stripping

Adapted from a published assay (Takada et al., 2012), stratum corneum collected by tape stripping the skin surface (three serial 22-mm tape strips in duplicate per sampling data point, see Supplementary Figure S3) was cut and pooled in 750 μl methanol. Samples were then subjected to an ultrasonic bath (20 minutes) agitated at 4 °C (20 minutes) filtered using a 0.2 μm syringe filter and dried. Distilled water (200 μl) was used to resuspend samples before analysis. Isocratic elution of pyrrolidine carboxylic acid (peak at 210 nm) and urocanic acid (peak at 270 nm) was performed in 0.1 M phosphate buffer (pH 2.75) containing 1% acetonitrile using a Shimadzu high-performance liquid chromatography system (Shimadzu, Kyoto, Japan) equipped with Synergi Hydro RP column (Phenomenex, Macclesfield, United Kingdom). A sample volume of 25 μl was injected in duplicate. The same extract was used to quantify the total free amino acid pool by o-phthaldehyde derivatization in triplicate (Nakagawa et al., 2004). Quantification of each NMF component was achieved by standard curve interpolation. The sum of all components (free amino acid pool, pyrrolidine carboxylic acid, and urocanic acid) was calculated and normalized relative to the amount of stratum corneum removed by tape stripping (Voegeli et al., 2007) to produce a single composite measure of NMF.

FLG genotyping

Genomic DNA was extracted from buccal swabs using the QIAamp DNA mini kit (Qiagen, Hilden, Germany). The four common European mutations were screened by Taqman (R501X and 2282del4) or sequencing (R2447X and S3247X) using established primer and probe sets (Sandilands et al., 2007).

Chemometric modeling

To evidence regions of infrared absorption by NMF components in vitro, chemicals were purchased from Sigma (Merck Life Science UK, Dorset, United Kingdom) dissolved in water at the following mole percent: serine, 31%; glycine, 16%; pyrrolidine carboxylic acid, 13%; histidine, 8%; citrulline, 6%; ornithine, 6%; threonine, 6%; urocanic acid, 4%; arginine, 3%; alanine, 3%, and analyzed using the same spectrometer. For the in vivo quantification of NMF by Attenuated Total Reflectance Fourier Transform Infrared spectroscopy, partial least squares regression modeling using the chemometrics software package Microlab Expert (Agilent Technologies) was employed to calibrate infrared absorption across the fingerprint spectral region (1,090–1,653 cm^{-1}) using a single, composite, quantitative measure of NMF (see NMF laboratory analysis ex vivo by tape stripping discussed earlier). For each volunteer, four sampling data points consisting of Infrared Spectroscopy performed before tape stripping were entered into the modeling, split equally between calibration and validation sets (Supplementary Figure S1). Four spectral repeats were averaged for each sampling data point. Before modeling, all spectra were normalized relative to amide III at 1,245 cm^{-1} (Zhang et al., 2006).

Statistical analysis

Results were collated in Excel, and all tests performed using GraphPad Prism 9 (GraphPad Software, San Diego, CA). Group means were compared using a Student's *t* test. The coefficient of determination assessed the linear regression model fit of ex vivo and in vivo NMF. Discrimination of atopic dermatitis phenotype and *FLG* loss-of-function genotype by in vivo modeled NMF was explored using binary logistic regression and receiver operating characteristic curve.

SUPPLEMENTARY REFERENCES

Nakagawa N, Sakai S, Matsumoto M, Yamada K, Nagano M, Yuki T, et al. Relationship between NMF (lactate and potassium) content and the physical properties of the stratum corneum in healthy subjects. J Invest Dermatol 2004;122:755–63.

Sandilands A, Terron-Kwiatkowski A, Hull PR, O'Regan GM, Clayton TH, Watson RM, et al. Comprehensive analysis of the gene encoding filaggrin uncovers prevalent and rare mutations

in ichthyosis vulgaris and atopic eczema. Nat Genet 2007;39:650–4.

Takada S, Naito S, Sonoda J, Miyauchi Y. Noninvasive in vivo measurement of natural moisturizing factor content in stratum corneum of human skin by attenuated total reflection infrared spectroscopy. Appl Spectrosc 2012;66:26–32.

Voegeli R, Rawlings AV, Doppler S, Heiland J, Schreier T. Profiling of serine protease activities in human stratum corneum and detection of a stratum corneum tryptase-like enzyme. Int J Cosmet Sci 2007;29:191–200.

Williams HC, Burney PG, Pembroke AC, Hay RJ. The U.K. Working Party's diagnostic criteria for atopic dermatitis. III. Independent hospital validation. Br J Dermatol 1994;131:406–16.

Zhang G, Moore DJ, Mendelsohn R, Flach CR. Vibrational microspectroscopy and imaging of molecular composition and structure during human corneocyte maturation. J Invest Dermatol 2006;126:1088–94.

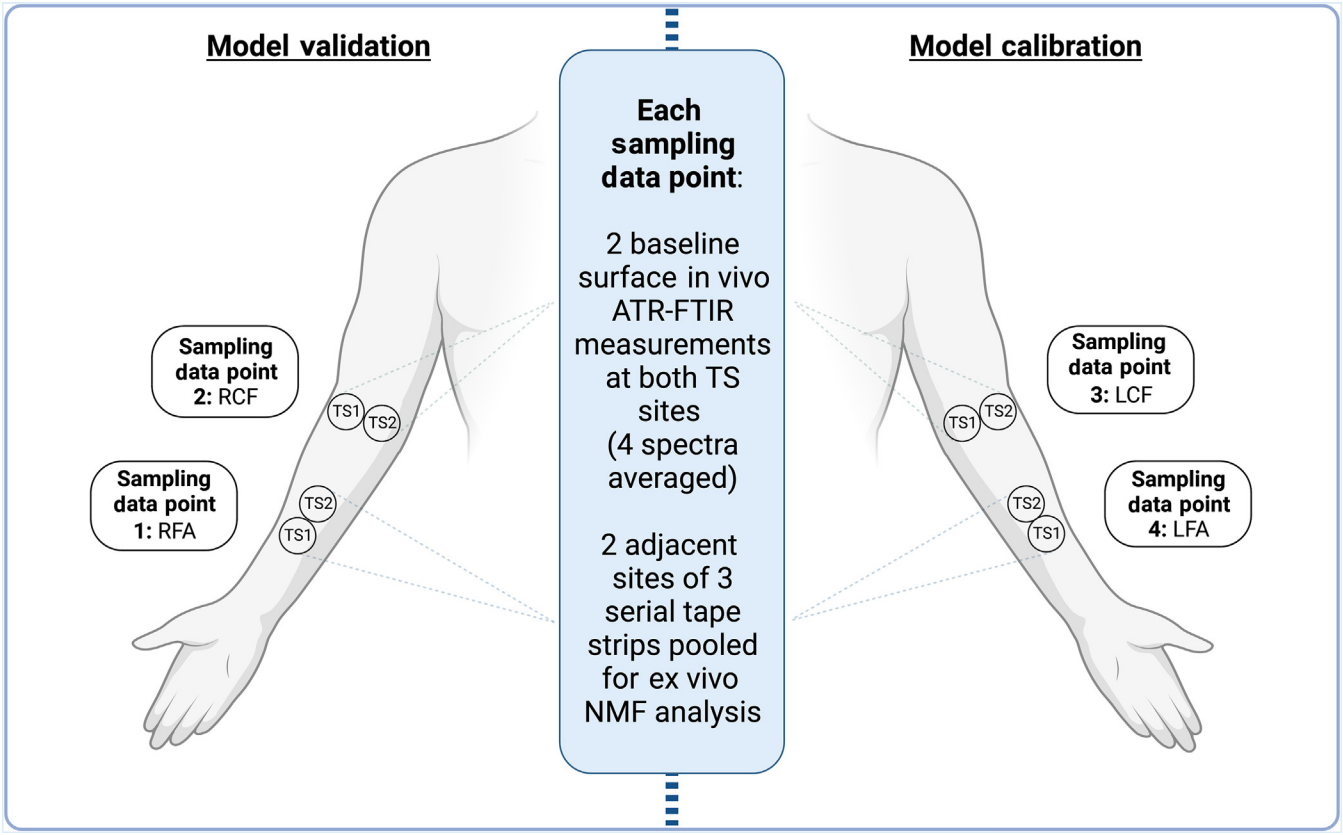

Supplementary Figure S1. Overview of the model build. ATR-FTIR, Attenuated Total Reflectance Fourier Transform Infrared Spectroscopy; LCF, left antecubital fossa; LFA, left forearm; RCF, right antecubital fossa; RFA, right forearm; TS, tape stripping.

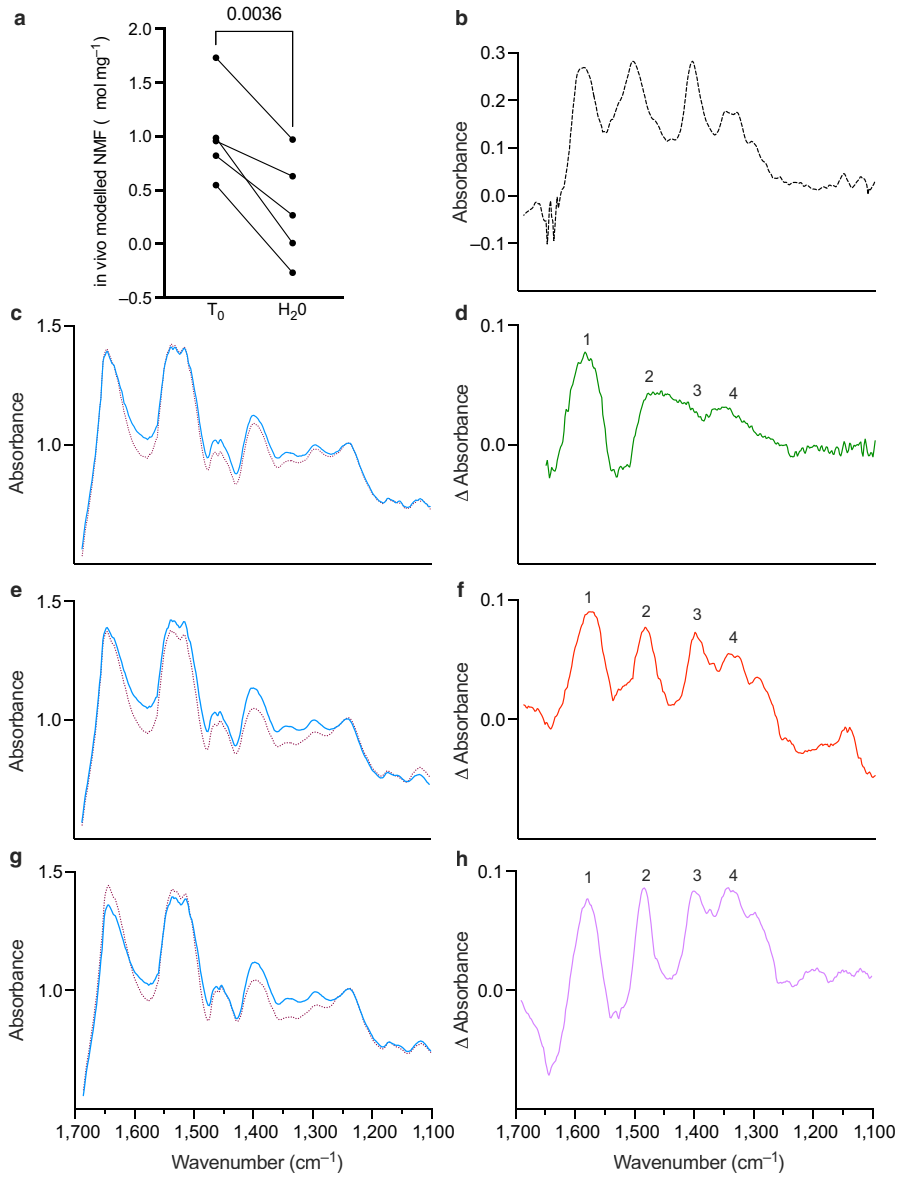

Supplementary Figure S2. Correlating spectral regions with NMF abundance. (**a**) In vivo modeled NMF before (T_0) and after (H_2O) soaking the antecubital fossa with water (20 minutes) in an additional cohort of five healthy volunteers. A significant reduction in NMF was observed using a paired Student's *t* test. (**c**) Mean ATR-FTIR spectra and (**d**) mean difference spectra (T_0−H_20) showing the changes in absorbance after the water soak. (**e**) Mean ATR-FTIR spectra and (**f**) mean difference spectra (n = 26) at the antecubital fossa obtained from healthy subjects (blue line) and AD subjects (red dotted line). (**g**) Mean ATR-FTIR spectra and (**h**) mean difference spectra (n = 26) at the antecubital fossa obtained from wild-type carriers (blue) and *FLG* LOF variants (red dotted line). Consistent changes in absorption were observed around (i) 1,580 cm^{-1}, (ii) 1,480 cm^{-1}, (iii) 1,400 cm^{-1}, and (iv) 1,340 cm^{-1} that correspond to (**b**) an in vitro spectrum of NMF. AD, atopic dermatitis; ATR-FTIR, Attenuated Total Reflectance Fourier Transform Infrared Spectroscopy; H_2O, water; LOF, loss-of-function; NMF, natural moisturizing factor.

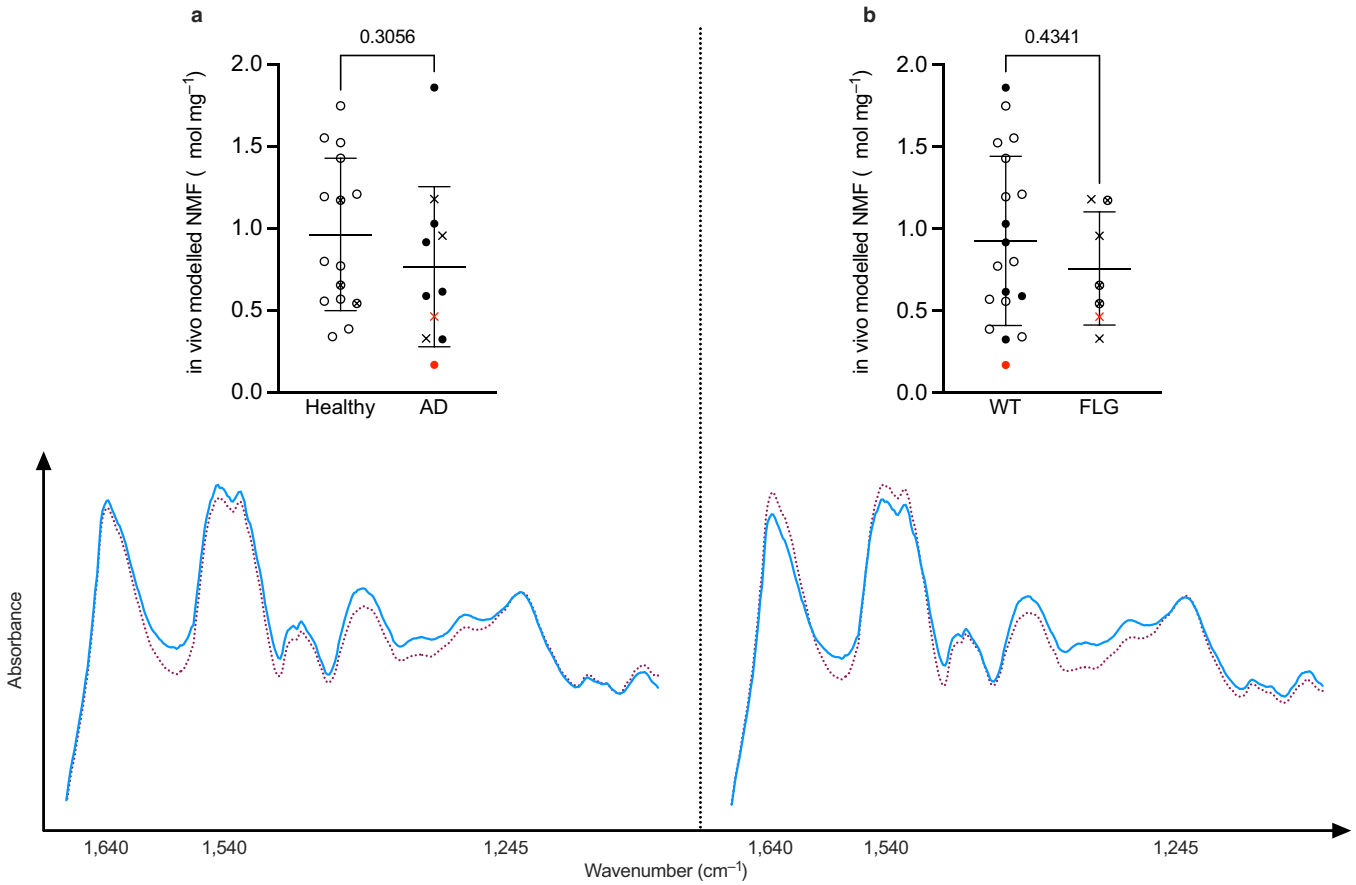

Supplementary Figure S3. Evaluation of in vivo modeled surface NMF at the forearm. No significant difference in mean NMF was found at the forearm using an unpaired Student's *t* test for (**a**) healthy compared with AD and (**b**) wild type compared with *FLG* LOF variants. Corresponding mean ATR-FTIR spectra are shown below each graph. Blue line = healthy (left) and WT (right). Red dotted line = AD (left) and *FLG* LOF variants (right). Please refer to Figure 1 for the key. AD, atopic dermatitis; LOF, loss-of-function; NMF, natural moisturizing factor; WT, wild type.

Supplementary Table S1. Study Cohort Characteristics

Characteristics	Healthy	AD	*P*-Value
N	15	11	
Age (y)	37 ± 14	36 ± 13	—
Sex (% female)	66	45	—
TEWL (g/m^2/hour)[1]	13.17 ± 3.05	14.52 ± 4.21	0.37
Capacitance (units)[1]	33.71 ± 6.83	29.48 ± 7.12	0.14
EASI score[2]	—	2.53 ± 0.39	—
FLG LOF (%)[3]	3/15 (20)	4/11 (36)	—
NMF (μmoles mg^{-1})[1,4]	1.28 ± 0.67	0.77 ± 0.25	**0.02**
fAA (μmoles mg^{-1})[1,4]	1.05 ± 0.53	0.66 ± 0.22	**0.04**
PCA (μmoles mg^{-1})[1,4]	0.18 ± 0.11	0.08 ± 0.03	**0.01**
UCA (μmoles mg^{-1})[1,4]	0.05 ± 0.03	0.03 ± 0.01	**0.03**
SC mass (mg^{-1})[5]	0.47 ± 0.08	0.45 ± 0.05	0.63

Abbreviations: AD, atopic dermatitis; EASI, Eczema Area and Severity Index; fAA, free amino acid pool; LOF, loss-of-function; NMF, natural moisturizing factor; PCA, pyrrolidone carboxylic acid; SC, stratum corneum; TEWL, transepidermal water loss; UCA, urocanic acid.

P-values denote the result of an unpaired Student's *t* test to compare groups. Significant results shown in bold. Mean ± SD is presented.

[1]Averaged across all sampling data points per person (see Supplementary Materials and Methods).

[2]Whole-body EASI scores averaged from two individuals with active AD.

[3]Carrying at least one *FLG* LOF allele.

[4]Ex vivo laboratory quantification of fAA, PCA, and UCA from tape strips. NMF is the sum of these three components.

[5]Cumulative mass of SC removed by tape stripping determined by densitometry averaged across all sampling data points.

Supplementary Table S2. Model Outputs Using Alternative Amide Normalization Modes

	1,640 cm^{-1} Normalization				1,540 cm^{-1} Normalization			
Model Output	**Healthy**	**AD**	**WT**	***FLG***	**Healthy**	**AD**	**WT**	***FLG***
Calibration (R^2)		0.72				0.71		
Validation (R^2)		0.72				0.71		
In vivo NMF FA site 1 (μmol mg^{-1})	0.97	0.70	0.91	0.71	0.97	0.71	0.90	0.77
In vivo NMF CF site 2 (μmol mg^{-1})	1.38	0.74[1]	1.27	0.66[2]	1.37	0.73[1]	1.25	0.71[2]

Abbreviations: AD, atopic dermatitis; CF, antecubital fossa; FA, forearm; LOF, loss-of-function; NMF, natural moisturizing factor; WT, wild type.

Asterisks denote the result of an unpaired Student's *t* test to compare groups (healthy/AD and WT/*FLG* LOF mutation carriers).

[1]P=<0.05 healthy compared to AD.

[2]$P = 0.05$ WT compared to *FLG* LOF variants.